CHAPTER VI
INFLUENCES OF A LIQUID CRYSTALLINE POLYMER, VECTRA A950, ON CRYSTALLIZATION KINETICS AND THERMAL STABILITY OF POLY(TRIMETHYLENE TEREPHTHALATE)

6.1 Abstract

The non-isothermal crystallization behavior of poly(trimethylene terephthalate) (PTT) and its blends with a liquid crystalline polymer, namely Vectra A950 (VA), was studied by differential scanning calorimetry. The values of the half-time of crystallization, $t_{0.5}$, and the parameter F(T) in the combined Avrami and Ozawa equation indicated that VA can enhance the PTT crystallization rate by acting as a nucleating agent. The crystallization activation energy of the PTT phase increased with increasing VA content. The blends were immiscible, as can be inferred from their morphology. Thermogravimetric analysis of the blends revealed the improved thermal stability by the incorporation of VA.

Key words: Differential Scanning Calorimetry; Liquid Crystalline Polymer; Non-Isothermal Crystallization Kinetics; Poly(trimethylene terephthalate)

6.2 Introduction

Thermotropic liquid crystalline polymers (LCPs) possess beneficial properties, such as high strength, high stiffness, and excellent barrier properties. Nonetheless, LCPs are still of limited use because of their high price. To achieve the advantages of the LCP properties simultaneously with economically attractive products, blending of LCP with a thermoplastic polymer has become an interesting choice. LCP/thermoplastic blends offer the potential of improved melt processibility and enhanced mechanical properties. Both

benefits arise from the unique rheological properties of LCP – under optimized flow conditions, they can align themselves and elongate to the direction of flow, resulting in a reduction in melt viscosity and superior mechanical properties [1–4]. Since the resulting physical properties are also strongly dependent on the extent of crystallization occurring during processing, studies related to the kinetics of polymer crystallization are therefore of great importance. There have been contradictory results regarding the effect of Vectra A950 (VA), a liquid crystalline polymer, on the crystallization kinetics of poly(ethylene terephthalate) (PET). To name a few, it has been shown that VA has a nucleating effect on PET crystallization [5,6]. On the other hand, it has also been reported that there is no evidence in favor of a nucleating effect of VA [7,8]. Magagnini et al. [9] studied the phase behavior of blends of PET with different LCPs, including VA, and claimed that all LCPs retarded the dynamic crystallization of PET. The conflicting results obtained so far lead to a requirement for further investigation of the crystallization kinetics of binary blends of VA with other terephthalate-based polyesters.

In this article, studies on PTT/VA blends under non-isothermal conditions were conducted by differential scanning calorimetry (DSC). The effects of VA on the crystallization kinetics of PTT were analyzed based on the combined Avrami and Ozawa model. The activation energies were calculated according to the Takhor model. Thermogravimetric analysis (TGA) was conducted, and the morphology of the blends was studied by scanning electron microscopy.

6.3 Experimental

6.3.1 Materials

Poly(trimethylene terephthalate) (PTT) was supplied, in pellet form, by PTT PolyCanada LP (Corterra 9200). Its intrinsic viscosity (IV) was 0.92 dl/g. The LCP used was Vectra A950 (labeled VA hereafter) and was supplied by Hoechst-Celanese. VA is a copolyester of 73 mol % p-hydroxybenzoic acid (HBA) and 27 mol % 2-

hydroxy-6-naphthoic acid (HNA). The materials were dried in a vacuum oven at 130°C for at least 12 h prior to use.

6.3.2 Preparation of Blends

PTT and VA resins were premixed in a dry mixer to prepare PTT/VA blends with VA contents of 0, 10, 30, and 70 wt%. The samples were designated as follows: VA wt %; for example, a blend containing 10 wt% VA and 90 wt% PTT would be called VA10. The dry-mixed blends were melt-mixed in a self-wiping, co-rotating twin-screw extruder (Collin, ZX-25). The temperature of the barrel section from the feeding zone to the die was set at 80, 230, 250, 275, 285, and 265°C. The rotor was operated at 30 rpm. The extrudates were cooled by water and then pelletized.

6.3.3 Differential Scanning Calorimetry (DSC) Procedures

The non-isothermal crystallization behaviors of the neat PTT and PTT/VA blends were analyzed using a Mettler-Toledo DSC822e differential scanning calorimeter (DSC). Each sample holder was loaded with samples of comparable quantity (6 ± 0.5 mg). The experiments were performed under dry nitrogen atmosphere starting with heating each sample from 25°C at a heating rate of 80°C/min to a fixed melt-annealing temperature of 310°C for 5 min in order to ensure complete melting. Then, each sample was cooled at cooling rates ranging from 10 to 30°C/min, to 120°C. The non-isothermal melt crystallization exotherms, the initial crystallization temperature (T_{ci}), the peak crystallization temperature (T_{cp}), the final crystallization temperature (T_{cf}), the half-time of crystallization ($t_{0.5}$), and the heat of crystallization (ΔH_c) were recorded. ΔH_c values were then normalized by the weight percent of a certain component to yield ΔH^*_c.

6.3.4 Thermogravimetric Analysis

Thermogravimetric analysis (TGA) was carried out using a Perkin Elmer TGA7 in the temperature range of 30 to 800°C, with a heating rate of 10°C/min under

nitrogen atmosphere. Decomposition temperature and the weight percent of the residue were recorded.

6.3.5 Morphological Study

The blend pellets were extruded through a capillary die with the inner diameter and the length of 1 and 20 mm (i.e. L/D ratio = 20), respectively, at 270°C, and a shear rate of 400 s^{-1} using a CEAST Rheologic 5000 twin-bore capillary rheometer. The morphology of the extruded fibers was examined through the observation of their fractured surfaces with a scanning electron microscope (JEOL JSM5200).

6.4 Results and Discussion

6.4.1 Non-Isothermal Melt Crystallization Behavior

Figure 6.1 shows the non-isothermal melt crystallization exotherms for blends with various VA contents at a cooling rate of 10°C/min, and Figure 6.2 shows the non-isothermal crystallization exotherms of VA70 at cooling rates ranging from 10 to 30°C/min. The exothermic peak occurring at lower temperature is ascribed to the melt crystallization peak of PTT, whereas the one at higher temperature represents that of VA. The VA peak, however, was too weak to be properly displayed for blends with a VA content of less than 70 wt%. From Table 6.1, all parameters regarding the peaks of PTT are indicated by the subscript (I) and those of VA by the subscript (II). According to the T_{cp} values, every sample crystallization peak shifts to lower temperature with increasing cooling rate. When the effect of VA content is considered, the $T_{cp(I)}$ values follow the order VA30 > VA10 > VA70 > VA0 at a fixed cooling rate. The higher T_{cp} infers a faster initiation of the melt crystallization process.

For non-isothermal crystallization, the relationship between time t and temperature T is expressed as:

$$t = \frac{|T_0 - T|}{\phi}, \qquad (6.1)$$

where T is the temperature at time t and ϕ is the cooling rate. The relative degree of crystallinity, X(T), as a function of temperature can be defined as:

$$X(T) = \frac{\int_{T_0}^{T} dH_c(T)/(dT)dT}{\int_{T_0}^{T_\infty} dH_c(T)/(dT)dT}, \qquad (6.2)$$

where T_0 and T_∞ are the initial and final crystallization temperature, respectively. The relative degree of crystallinity as a function of time is shown in Figure 6.3. The half-time of crystallization ($t_{0.5(I)}$) has been defined as the time required to attain half of the final degree of crystallinity and was used to rank the crystallization rate: the lower the $t_{0.5}$, the higher the crystallization rate. The obtained $t_{0.5(I)}$ values are mostly ranked as follows: VA0 > VA70 > VA30 ≈ VA10 (see Table 6.1). Therefore, the presence of VA can enhance the melt crystallization process of PTT. However, at a very high VA content, like VA70, the rate of the melt crystallization process of PTT is lower than VA10 and VA30 due to the dilution of PTT concentration upon blending with VA. This leads to difficulties in the transport process of PTT segments to the crystallite–melt interface in VA70, which will be confirmed by the crystallization activation energy values (see later). For the VA phase, changes in PTT content do not significantly alter either $T_{cp(II)}$ or $t_{0.5(II)}$, indicating a negligible effect of PTT on the VA crystallization rate. This might arise from the fact that the PTT phase still remains in its melting state in the temperature range in which VA crystallizes (PTT melts at ~227°C). Therefore, the presence of PTT neither effectively impedes the VA chain mobility nor acts as a nucleating agent, and thus this work focuses on the influence of VA on the PTT crystallization rate only.

The normalized crystallization enthalpy can be used to rank the crystallization extent during melt crystallization. As shown in Table 6.1, $\Delta H^*_{c(I)}$ values (the enthalpies related to the PTT phase) are mostly in the following order: VA10 > VA30 > VA0 > VA70. There are two main reasons for an increase in $\Delta H^*_{c(I)}$: first, the addition of VA can increase the crystallization temperature, which results in a longer crystallization time; second, the addition of VA increases the rate of crystallization, as reflected in the values of $t_{0.5(I)}$. From both reasons, VA10 and VA30 exhibit higher

$\Delta H^*_{c(I)}$ than VA0 and VA70, respectively. However, the incorporation of a very high VA content might result in smaller size and less perfection of the PTT crystallites, yielding a lower crystallization extent. Sharma et al. [5] postulated that, at high VA content, the excessive nucleation at the polymer interface leads to an imperfect crystal formation, thus lowering the extent of crystallization. This could probably account for the faster crystallization rate but lower crystallization extent of VA70 compared to those of VA0. In the case of $\Delta H^*_{c(II)}$ (the normalized crystallization enthalpy belonging to the VA fraction), the crystallization extent of VA70 is higher than that of VA30. Thus, a too high PTT content can in turn result in smaller crystallite size and less perfect VA crystallites.

6.4.2 Non-Isothermal Crystallization Kinetics

Isothermal crystallization is an idealized crystallization process, well described by the Avrami theory [10]. The Avrami approach, therefore, ignores the effects of cooling rate and thermal gradients within the sample and is expressed as:

$$\log[-\ln(1-X_t)] = \log Z_t + n\log t, \qquad (6.3)$$

where X_t is the relative degree of crystallinity, n is the Avrami exponent that depends on the nucleation and growth process, t is the time, and Z_t is the rate constant. In order to make this model applicable to the non-isothermal crystallization process, Jeziorny [11] introduced the cooling rate, ϕ , to correct the crystallization rate constant:

$$\log Z_c = \frac{\log Z_t}{\phi}. \qquad (6.4)$$

Also, Ozawa [12] modified the equation by introducing the effect of the cooling rate, assuming that the non-isothermal crystallization process is composed of infinitesimally small isothermal crystallization steps:

$$\log[-\ln(1-X_t)] = \log K(T) - m\log\phi, \qquad (6.5)$$

where $K(T)$ is the function of cooling rate, m is the Ozawa exponent, similar to the Avrami exponent, and ϕ is the cooling rate. Mo and coworkers [13] proposed a novel

kinetics equation by combining Equations 6.3 and 6.5; at a certain degree of crystallinity, X_t, the following equation can be obtained:

$$\ln \phi = \ln F(T) - a \ln t, \qquad (6.6)$$

where

$$F(T) = [K(T)/Z_t]^{1/m} \text{ and } a = n/m.$$

The physical meaning of $F(T)$ is the necessary cooling rate when the measured system arrives at a certain relative degree of crystallinity at unit crystallization time, which is related to the difficulty of the crystallization process for that particular material. According to Equation 6.6, at a given degree of crystallinity, the plot of $\ln \phi$ as a function of $\ln t$ should yield a straight line with $\ln F(T)$ as the intercept and $-a$ as the slope. Plots of $\ln \phi$ versus $\ln t$ at various relative degrees of crystallinity for the neat PTT and the PTT/VA blends during non-isothermal crystallization show a good linear relationship, verifying that this combined Avrami–Ozawa equation is applicable to these systems (see Figure 6.4 for the plots of the neat PTT).

The values of $F(T)$ and a are listed in Table 6.2. Obviously, the values of $F(T)$ generally increase with increasing relative crystallinity, suggesting that, at a unit crystallization time, a higher cooling rate was required to obtain a higher degree of crystallinity. The values of $F(T)$ are in the following sequence: VA0 > VA70 > VA10 > VA30. This sequence represents the necessary cooling rate for each sample to arrive at the same degree of crystallinity for a given unit crystallization time. In other words, the crystallization rates are in the following order: VA30 > VA10 > VA70 > VA0. The values of the parameter a range from 1.22 to 2.33 and are found to be fairly constant for each sample.

6.4.3 Determination of the Crystallization Activation Energy

In this paper, the Takhor [14] model was employed to determine the crystallization activation energy for the transport of PTT chains towards the growing surface. The crystallization activation energy (ΔE) is defined as follows:

$$\frac{d[\ln \phi]}{d[1/T_{cp}]} = -\frac{\Delta E}{R} \tag{6.7}$$

where R is the universal gas constant. The good linearity of the plots of $\ln \phi$ versus $1/T_{cp}$ is displayed in Figure 6.5. The ΔE values were calculated from the slopes of the plots [i.e. ΔE = -(slope)(R)] and are listed in Table 6.3. The higher the absolute ΔE value, the more difficult the transport of polymer chains to a growing crystal surface. It is clear that the absolute ΔE values increase with increasing VA content, suggesting that although VA can act as a nucleating agent, it can in turn hinder the transport of the polymer chains. Since crystallization includes two processes, nucleation and growth, the addition of VA, which has a positive effect on the nucleation process and a negative effect on the growth process, results in a net positive effect on the non-isothermal crystallization rate throughout the compositions studied.

6.4.4 Thermal stability of PTT/VA Blends

The TGA curves of the neat polymers and the blends obtained at a heating rate of 10°C/min in N_2 are shown in Figure 6.6. From the thermograms, PTT/VA shows a two-step decomposition. The first step corresponds to the decomposition of the PTT component, whereas the second corresponds to the VA component. In this paper, the decomposition temperature ($T_{d,w}$) is defined, according to Wright [15], as the temperature at which the weight of a polymer decreases by 1% during the heating scan. Both T_d values and residue content are greater as VA content increases (see Table 6.4). Thus, VA can improve the thermal stability of the blends.

6.4.5 Morphology of PTT/VA Blends

Figures 6.7 (a)–(c) are SEM micrographs of the fractured surfaces of the blends. It is clear that all the blends reveal a biphasic morphology typical of highly immiscible blends. The dispersed VA domains are both spherical and fibrillar. These domains are enlarged with increasing VA content as a result of phase coalescence. Interestingly, at a VA content as high as 70 wt%, the VA phase does not become the

matrix, but forms thick, continuous fibrils surrounded by the PTT matrix. This implies a large difference in viscosity between the two phases.

6.5 Conclusions

The non-isothermal crystallization behaviors of poly(trimethylene terephthalate) (PTT) and its blends with Vectra A950 (VA) were investigated. An increase in the PTT melt crystallization temperature was ascribed to the nucleation effect of VA. The values of half-time of crystallization, $t_{0.5}$, and the parameter F(T) in the combined Avrami–Ozawa equation confirmed that the non-isothermal crystallization rate of PTT was enhanced in the presence of VA for all compositions studied. TGA results suggest improved thermal stability by the incorporation of VA. The observed biphasic morphology implied the immiscibility of all the blends. Both fibrillar and spherical VA domains were observed at low VA content. At the VA content of 70 wt%, all the VA domains were found to be in the form of large fibrils.

6.6 Acknowledgements

The authors are grateful for the financial support of the Royal Golden Jubilee Ph.D. Program (Thailand). domains were found to be in the form of large fibrils.

6.7 References

1 T. Rath, S. Kumar, R. N. Mahaling, M. Mukherjee, C. K. Das, K. N. Pandey and A. K. Saxena, J. Appl. Polym. Sci., 104 (2007) 3758-3765.

2 J. Chen, P. Chen, L. Wu, J. Zhang and J. He, Polymer 48 (2007) 4242-4251.

3 A. K. Kalkar, A. A. Deshpande and M. J. Kulkarni, J. Appl. Polym. Sci., 106 (2007) 34-45.

4 T. Rath, S. Kumar, R. N. Mahaling, C. K. Das and S. B. Yadaw, J. Appl. Sci., 106 (2007) 3721-3728.

5 S. K. Sharma, A. Tendolkar and A. Misra, Mol. Cryst. Liq. Cryst., 157 (1988) 597-614.

6 D. Melot and W. J. MacKnight, Polym.Adv. Technol., 3 (1992) 383-388.

7 G. P. Chang-Chien and M. M. Denn, Polym. Adv. Technol., 7 (1996) 168-172.

8 W. N. Kim and M. M. Denn, J. Rheol., 36 (1992) 1477-1498.

9 P. L. Magagnini, M. S. Tonti, M. Masseti, M. Paci, L. I. Minkova and T. S. Miteva, Polym. Eng. Sci., 38 (1998) 1572-1586.

10 M. Avrami, J. Chem. Phys., 8 (1940) 212-224.

11 A. Jeziorny, Polymer, 19(10), (1978) 1142-1144.

12 T. Ozawa, Polymer, 12 (1971) 150-158.

13 J. P. Liu, Z. S. Mo, Y. C. Qi, H. F. Zhang and D. I. Chen, Acta. Polym. Sin., 1 (1993) 1-6.

14 R. L. Takhor, Advance in Nucleation and Crystallization of Glasses, American Ceramics Society, Columbus 1971, p.166.

15 J. Wright, Thermal degradation of polymers. Soc. Chem. Industries 13 (3) 1961, p. 248.

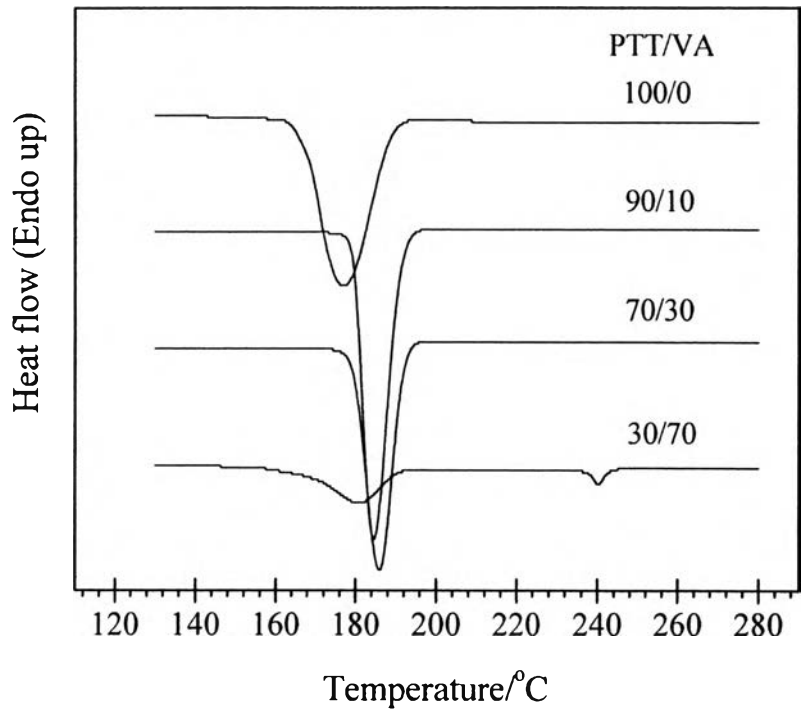

Figure 6.1 Non-isothermal melt crystallization exotherms for neat PTT and PTT/VA blends at a cooling rate of 10°C/min.

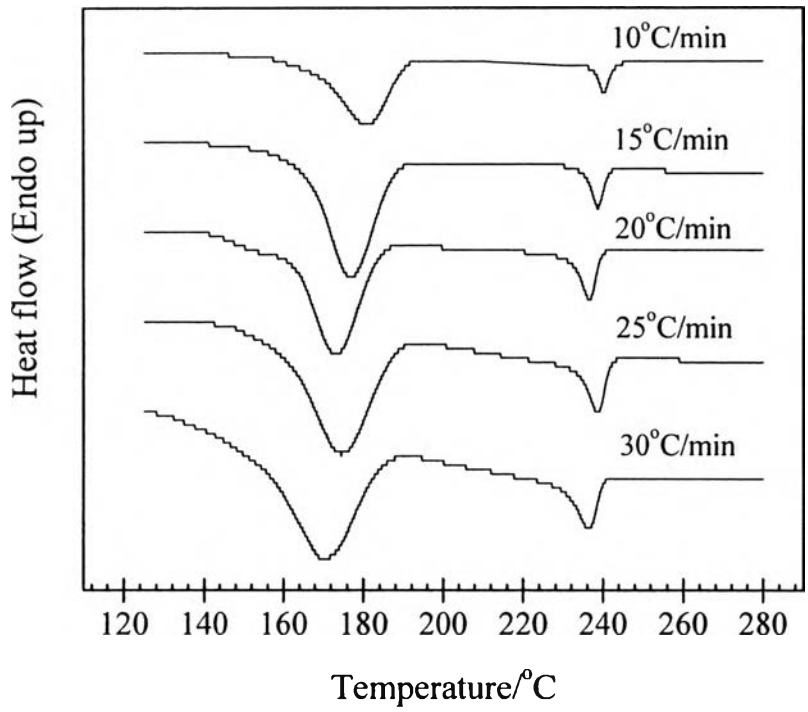

Figure 6.2 Non-isothermal melt crystallization exotherms for the VA70 blend at five different cooling rates ranging from 10 to 30°C/min.

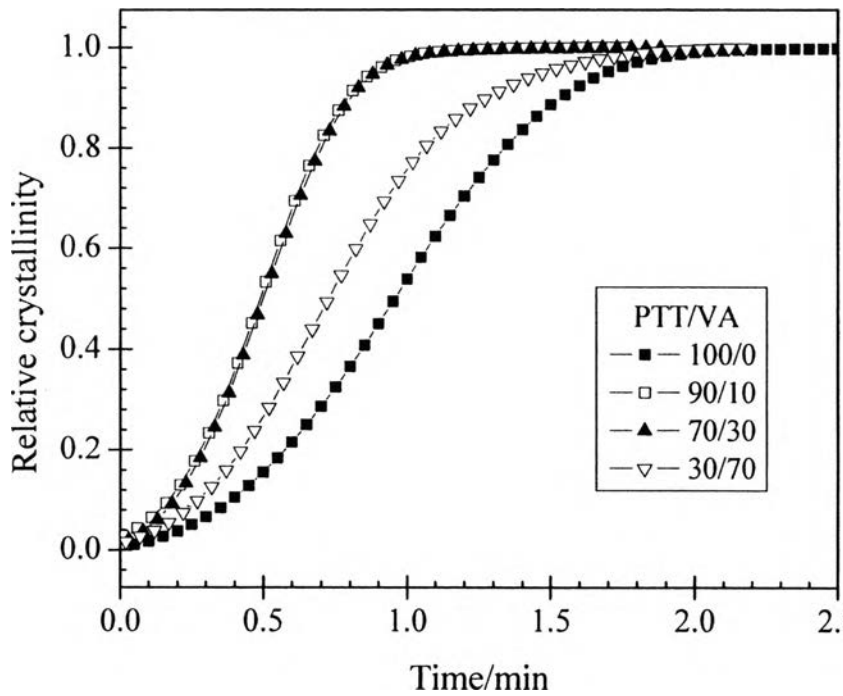

Figure 6.3 Relative crystallinity function of time of PTT and PTT/VA blends at a cooling rate of 15°C/min.

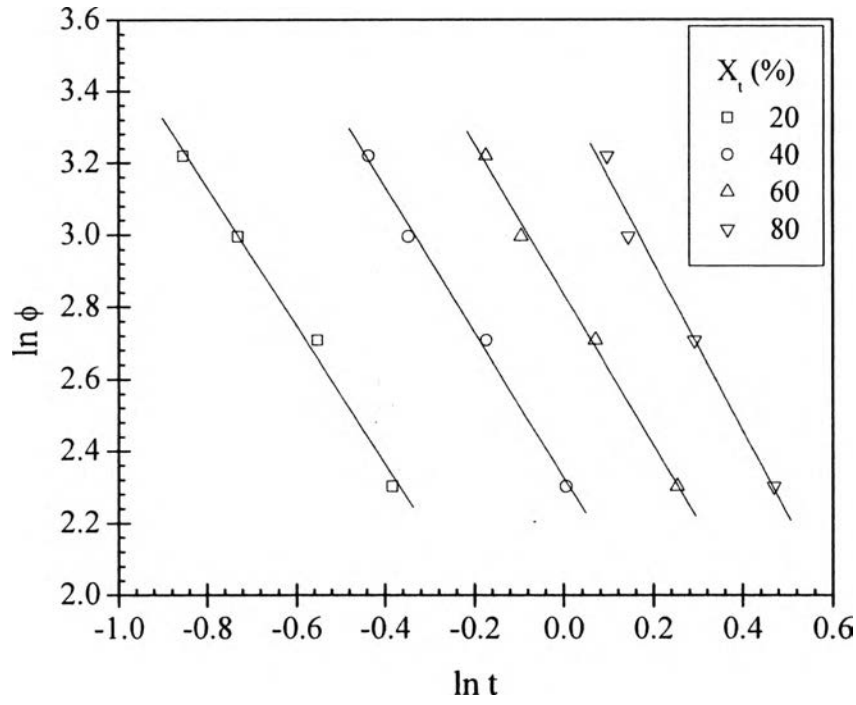

Figure 6.4 Plots of $\ln \phi$ versus $\ln t$ for neat PTT at various relative crystallinities.

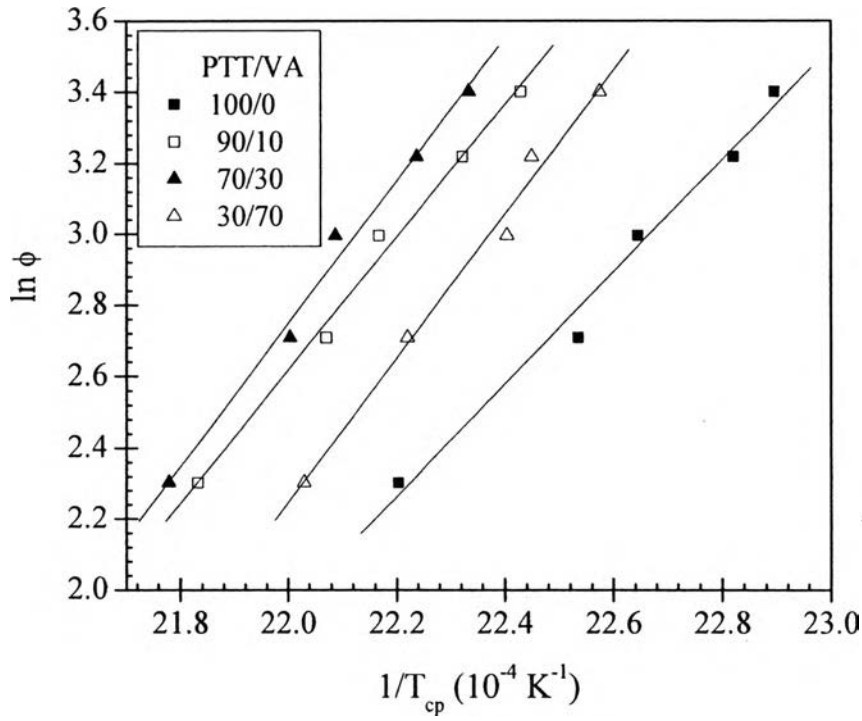

Figure 6.5 Plots of $\ln\phi$ versus $1/T_{cp}$ for neat PTT and their blends at various compositions.

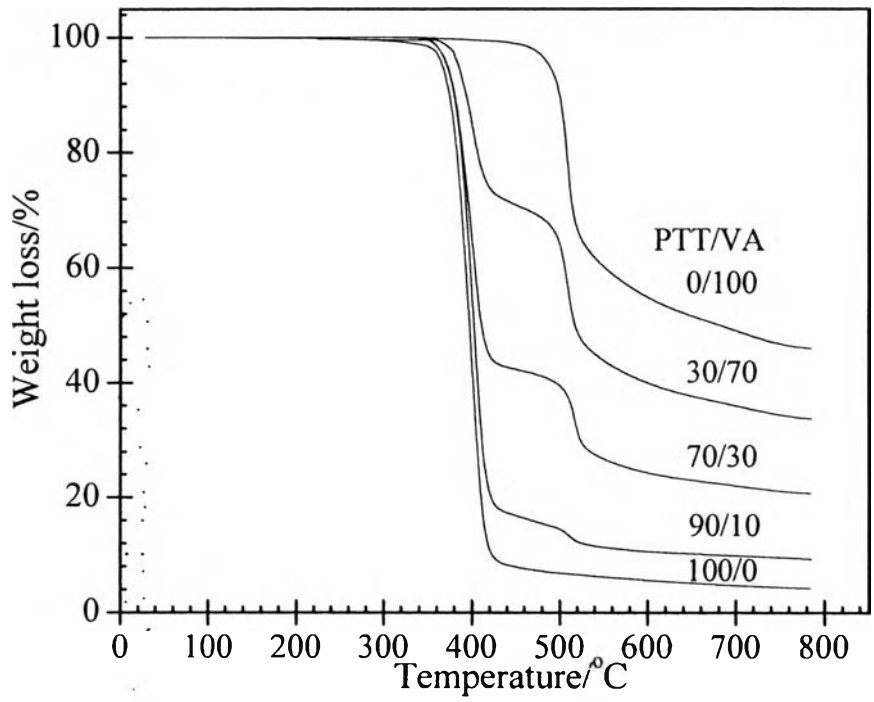

Figure 6.6 TGA thermograms of PTT, VA, and their blends.

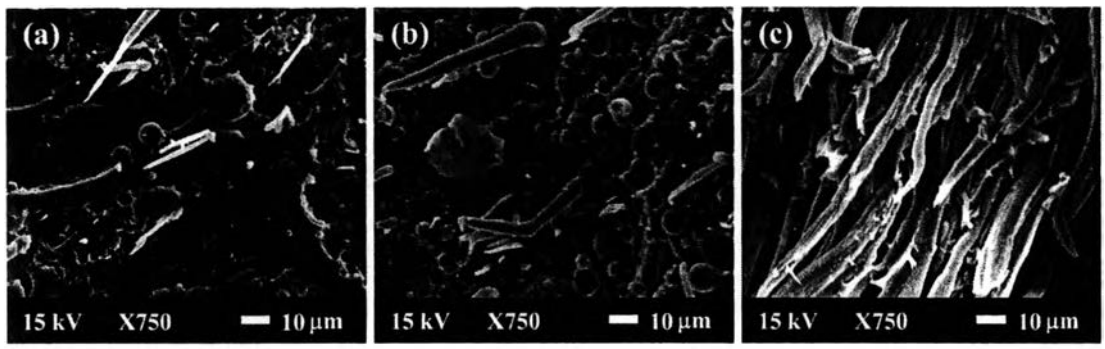

Figure 6.7 Scanning electron micrographs of Vectra/PTT strands extruded through a capillary with a constant strain rate of 400 s^{-1}, temperature 270°C, and Vectra contents of (a) 10, (b) 30, and (c) 70 wt%.

Table 6.1 Non-isothermal melt-crystallization data for the neat PTT, and PTT/VA blends at various cooling rates

ϕ /°C min^{-1}	Sample	$T_{ci(I)}$ /°C	$T_{cp(I)}$ /°C	$T_{cf(I)}$ /°C	$\Delta H_{c(I)}$ /J g^{-1}	$\Delta H^*_{c(I)}$ /J g^{-1}	$t_{0.5(I)}$ /s	$T_{ci(II)}$ /°C	$T_{cp(II)}$ /°C	$T_{cf(II)}$ /°C	$\Delta H_{c(II)}$ /J g^{-1}	$\Delta H^*_{c(II)}$ /J g^{-1}	$t_{0.5(II)}$ /s
10	VA0	188.9	177.2	167.1	60.20	60.20	71	-	-	-	-	-	-
	VA10	191.2	184.9	179.5	59.96	66.62	40	-	-	-	-	-	-
	VA30	191.9	186.0	179.4	45.76	65.37	37	244.2	240.7	237.2	0.62	0.89	21
	VA70	190.6	180.8	166.8	13.61	45.37	59	243.2	240.3	237.4	1.63	2.33	17
15	VA0	185.0	170.6	156.5	61.00	61.00	58	-	-	-	-	-	-
	VA10	187.3	180.0	172.8	58.60	65.10	31	-	-	-	-	-	-
	VA30	189.0	181.3	174.3	44.60	63.70	31	241.7	238.5	234.2	0.71	1.01	13
	VA70	187.5	176.9	165.8	13.90	46.30	42	241.8	238.9	235.2	1.65	2.36	12

ϕ /°C min^{-1}	Sample	$T_{ci(I)}$ /°C	$T_{cp(I)}$ /°C	$T_{cf(I)}$ /°C	$\Delta H_{c(I)}$ /J g^{-1}	$\Delta H^{*}_{c(I)}$ /J g^{-1}	$t_{0.5(I)}$ /s	$T_{ci(II)}$ /°C	$T_{cp(II)}$ /°C	$T_{cf(II)}$ /°C	$\Delta H_{c(II)}$ /J g^{-1}	$\Delta H^{*}_{c(II)}$ /J g^{-1}	$t_{0.5(II)}$ /s
20	VA0	184.2	168.4	152.1	57.27	57.27	47	-	-	-	-	-	-
	VA10	185.3	178.0	171.0	58.56	65.07	23	-	-	-	-	-	-
	VA30	186.2	179.6	169.4	43.68	62.40	29	240.5	237.2	231.6	0.50	0.71	13
	VA70	183.5	173.2	157.7	10.41	34.70	33	239.9	237.5	231.9	1.67	2.39	12
25	VA0	179.6	165.1	140.1	60.40	60.40	39	-	-	-	-	-	-
	VA10	183.0	174.8	166.5	54.87	60.97	20	-	-	-	-	-	-
	VA30	185.7	176.5	167.8	42.42	60.60	23	240.3	236.6	230.8	0.64	0.91	13
	VA70	187.6	174.5	159.5	12.19	40.63	32	242.2	237.0	232.9	1.85	2.64	12
30	VA0	179.4	163.6	146.0	61.40	61.40	32	-	-	-	-	-	-
	VA10	181.1	172.7	163.4	55.07	61.19	18	-	-	-	-	-	-
	VA30	184.5	174.6	165.4	42.17	60.24	20	239.9	236.3	229.4	0.76	1.09	7
	VA70	183.5	169.8	152.8	11.67	38.90	27	241.1	236.9	229.4	1.58	2.26	8

Table 6.2 Non-isothermal melt-crystallization kinetics parameters obtained from the combined Avrami–Ozawa approach at cooling rates ranging from 10 to 25°C/min

X(t)/%	VA0		VA10		VA30		VA70	
	F(T)	*a*	F(T)	*a*	F(T)	*a*	F(T)	*a*
20	4.95	1.91	2.37	1.40	1.59	1.87	5.60	1.27
30	8.07	1.70	3.29	1.43	2.26	1.93	7.61	1.26
40	10.24	2.02	4.25	1.41	3.09	1.93	9.43	1.25
50	13.76	1.91	5.11	1.42	4.04	1.91	11.32	1.25
60	17.01	2.09	5.99	1.43	5.11	1.89	13.41	1.23
70	21.96	2.19	6.91	1.44	6.38	1.85	15.98	1.22
80	29.67	2.33	8.09	1.46	7.51	1.92	20.17	1.26

Table 6.3 Crystallization activation energy of PTT, VA, and their blends

	PTT	VA10	VA30	VA70
ΔE /kJ mol^{-1}	-131.2	-155.2	-166.7	-168.4

Table 6.4 Decomposition temperatures of PTT, VA, and PTT/VA blends at 1% weight loss and residue at 700°C

PTT/VA/(wt/wt)	$T_{d,w}$/°C	Residue at 700°C/wt%
0/100	446.9	49.1
30/70	367.5	36.0
70/30	356.9	22.0
90/10	347.9	12.5
100/0	330.6	4.7